

$(\eta^5\text{-C}_5\text{Me}_5)_2\text{Yb}(\text{NC}_5\text{H}_5)_2$.²⁶ The Yb(2)–O(2) separation of 2.46 (3) Å is slightly longer than the 2.41 Å found for $(\eta^5\text{-C}_5\text{Me}_5)_2\text{Yb}(\text{OC}_4\text{H}_8)$.^{2a} Again, although the standard deviations are high, one would expect an increase of 0.06 Å in the ionic radius of eight-coordinate Yb(II) vs. seven-coordinate Yb(II).²⁷

It is unfortunate that the disorder in molecule 1 obscures the Yb(1)–N(1) distance but this important aspect of the structure is observed in the second molecule. Here, the Yb(2)–N(2) separation is 2.55 (3) Å. This short distance shows that the ammonia molecule is held tightly enough by the ytterbium metal to resist displacement by other donor solvents. A similar Yb–N distance of 2.56 Å has been found in $(\eta^5\text{-C}_5\text{Me}_5)_2\text{Yb}(\text{NC}_5\text{H}_5)_2$.²⁶

In conclusion, our results indicate that organolanthanoid synthesis in liquid ammonia is a viable alternate route to

standard metathetical schemes when appropriate cautions are exercised as to choice of substrate and reaction conditions.

Acknowledgment. We thank Cynthia Day of Crystallitics Co. for expeditious data collection, F. J. DiSalvo and J. V. Waszczak for magnetic susceptibility measurements, Prof. J. J. Dechter for the ¹³C NMR spectrum of $(\text{C}_5\text{Me}_5)_2\text{Yb}(\text{NH}_3)(\text{THF})$, and Prof. R. A. Andersen for helpful advice and discussion. We also wish to thank a reviewer for helpful editorial and content suggestions.

Registry No. $(\text{C}_5\text{Me}_5)_2\text{Yb}(\text{NH}_3)(\text{THF})$, 91443-87-7; $(\text{C}_5\text{Me}_5)_2\text{Eu}(\text{THF})$, 91443-88-8; Yb, 7440-64-4; Eu, 7440-53-1.

Supplementary Material Available: Schematic diagram of vacuum line and ancillary equipment and tables of thermal parameters, bond distances and angles, best plane results, and observed and calculated structure factors (25 pages). Ordering information is given on any current masthead page.

(26) Tilley, T. D.; Andersen, R. A.; Spencer, B.; Zalkin, A. *Inorg. Chem.* **1982**, *21*, 2647.

(27) Shannon, R. D. *Acta Crystallogr., Sect. A* **1976**, *A32*, 751.

Photochemistry and Electronic Structure of the $(\eta^5\text{-C}_5\text{H}_5)_2\text{MoS}_2$ Complex

Alice E. Bruce, Mitchell R. M. Bruce, Anthony Sclafani, and David R. Tyler*

Department of Chemistry, Columbia University, New York, New York 10027

Received March 21, 1984

The photochemistry of the Cp_2MoS_2 complex was studied in order to determine if d–d excited states gave different photochemistry than the $\text{S} \rightarrow \text{Mo}$ charge-transfer excited states. The various excited states were identified with the aid of a self-consistent field– $X\alpha$ –scattered-wave molecular orbital calculation. No wavelength dependent photochemistry was found as irradiation of the Cp_2MoS_2 complex in inert solvents at all selected wavelengths led to Cp_2MoS_4 . The mechanism of Cp_2MoS_4 formation was studied. Two pathways seemed likely: photochemical extrusion of either S_2 or S_2^{2-} . The formation of Cp_2MoS_4 does not necessarily imply the extrusion of S_2 rather than S_2^{2-} because the latter species can disproportionate: $2\text{S}_2^{2-} \rightarrow \text{S}_2 + 2\text{S}^{2-}$. In order to differentiate between homolytic and heterolytic Mo–S bond cleavage pathways, the Cp_2MoS_2 complex was irradiated in CDCl_3 . The products in this solvent are Cp_2MoCl_2 and Cp_2MoS_4 , at all wavelengths. Other unidentified minor products also formed in the photochemical reactions of the Cp_2MoS_2 . Since the reaction of molybdenocene with CHCl_3 produces Cp_2MoCl_2 and because attempts to trap $\text{Cp}_2\text{Mo}^{2+}$ failed, it is proposed that homolytic extrusion of S_2 follows irradiation of the Cp_2MoS_2 complex. Reasons for the wavelength independent photochemistry and for the homolytic extrusion of S_2 , upon irradiation in either the $14a_1 \rightarrow 9b_1$ d–d band (490 nm) or the $6a_2 \rightarrow 9b_1$ S \rightarrow Mo charge-transfer (420 nm) band, are discussed.

Introduction

In a recent paper we reported that S \rightarrow Ti charge-transfer excitation of the Cp_2TiS_2 complex led to homolytic cleavage of a Ti–S bond.¹ This result led us to pose two questions. First, was homolytic cleavage typical of S \rightarrow M CT excited states? And second, was this behavior characteristic only of S \rightarrow M CT excited states or will d–d excited states also lead to homolytic cleavage of S–M bonds in organometallic sulfide complexes? To answer these questions we decided to study the photochemistry of the Cp_2MoS_2 complex, a molecule with a d^2 configuration. The presence of d–d transitions allowed us to compare the reactivity of d–d excited states with the reactivity of the S \rightarrow M CT states.

In order to differentiate between the d–d and S \rightarrow M CT bands in the absorption spectrum of the Cp_2MoS_2 complex, we used the SCF– $X\alpha$ –SW molecular orbital

method to calculate the electronic structure of the complex. With the aid of the MO calculation we were able to assign the bands in the electronic spectrum of the complex. This paper reports the results of our molecular orbital study of the Cp_2MoS_2 complex and also the results of some photochemical reactions.

Experimental Section

SCF– $X\alpha$ –SW Procedure. Calculations were carried out by using the SCF– $X\alpha$ –SW method.² Current versions of the programs were used,³ and they were run on the chemistry department's DEC VAX 11/780 computer. Norman's procedure for interpolation of overlapping sphere sizes was used to optimize the virial coefficient at one.^{4,5} The electronic transition energies

(2) (a) Slater, J. C. "The Calculation of Molecular Orbitals"; New York, 1979 and references therein. (b) Johnson, K. H. *Adv. Quantum Chem.* **1973**, *7*, 143–185 and references therein. (c) Rosch, N.; Klemperer, W. G.; Johnson, K. H. *Chem. Phys. Lett.* **1973**, *23*, 149–154. (d) Johnson, K. H.; Smith, F. C. *Phys. Rev. B: Solid State* **1972**, *5*, 831–843.

(3) The programs were received from K. H. Johnson in 1981 and converted for use on a DEC VAX 11/780 by W. H. Klemperer and M. R. Bruce.

(1) Bruce, A. E.; Bruce, M. R. M.; Tyler, D. R., *J. Am. Chem. Soc.*, in press.

Table I. Relative Amounts of Products Formed by Irradiation

compd	solv	irradiation		% of products ^a			
		wavelength, nm	duratn, h	Cp ₂ MoS ₂	Cp ₂ MoS ₄	Cp ₂ MoCl ₂	ΣX ^b
Cp ₂ MoS ₂	C ₆ H ₆	λ > 470	3	76	8		16
Cp ₂ MoS ₂	C ₆ H ₆	λ > 350	1	40	9		51
Cp ₂ MoS ₄	C ₆ H ₆	λ > 470	3	25	60		15
Cp ₂ MoS ₂	CDCl ₃	λ > 530	1	72	12	5	11
Cp ₂ MoS ₂	CDCl ₃	λ > 430	1	42	19	11	28
Cp ₂ MoS ₂	CDCl ₃	λ > 350	1	18	16	19	47
Cp ₂ MoS ₄	CDCl ₃	λ > 530	1.5	10	73		17
Cp ₂ MoS ₄	CDCl ₃	λ > 350	1.5	5	62	6	27

^a Calculated from ¹H NMR peak integration (±10%). ^b Total contribution from all other unidentified resonances; see Experimental Section for more details.

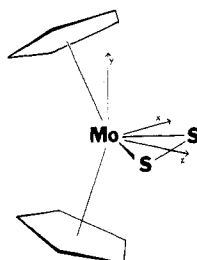


Figure 1. Coordinate system used in the SCF-X α -SW calculation on Cp₂MoS₂.

were calculated by using the unrelaxed SCF optical transition calculation. This involves taking the difference between energy levels of converged molecular orbitals.^{2b} It is our experience that the difference between unrelaxed SCF calculations and the Slater transition-state calculation is small for the Cp₂MX₂ organometallic molecules.⁶ Schwartz's α_{HF} values⁷ were used for the atomic exchange parameters, except for hydrogen in which case Slater's value⁸ of 0.777 25 was used. The α values for the inter-sphere and outer-sphere regions were a weighted average of the atomic α values, where the weights are the number of valence electrons on the different neutral free atoms.

A minimal basis set was used for all atoms except sulfur where $l = 2$.⁹ The use of a minimal basis set is justified on the basis of previous results.⁶ Using the value of $l = 2$ for the outer-sphere region was sufficient to generate basis function components in all representations.

The coordinates of the Cp₂MoS₂ complex had to be estimated because X-ray crystallographic data were not available. Figure 1 shows the coordinate system used for the Cp₂MoS₂ complex. All of the molecular coordinates were adjusted to idealized C_{2v} symmetry. The Cp-Mo, Mo-S, and S-S bond distances and angles were based on X-ray crystallographic data of several analogous complexes.¹⁰

Materials and Methods. All preparative and photochemical reactions were done under an argon or nitrogen atmosphere using a combination of vacuum line and Schlenk techniques, a Vacuum

Atmospheres drybox, and a glovebag. Benzene, chloroform, and carbon tetrachloride were certified ACS spectroanalyzed grade from Fisher Scientific. Benzene was dried over CaH₂ and distilled under nitrogen. Chloroform and carbon tetrachloride were dried over P₂O₅ and distilled under nitrogen.¹¹ Deuterated NMR solvents were obtained from Aldrich, except chloroform-*d* which was obtained from Norell Inc. Tetrabutylammonium chloride was obtained from Aldrich and recrystallized in the drybox from dry acetone and anhydrous ether. Sodium hydrogen sulfide was obtained from Alfa and used as received. Cp₂MoCl₂ was prepared according to a published procedure.¹²

Electronic absorption spectra were recorded on a Cary 17 spectrophotometer. Electronic spectra of Cp₂MoS₂ were obtained in benzene ($\lambda > 300$ nm) and acetonitrile ($\lambda > 210$ nm). ¹H NMR spectra were obtained on a Varian XL 200 or a Bruker WM 250 instrument. Peak assignments (δ) are relative to the appropriate solvent peak: CHCl₃, 7.27; C₆H₆, 7.15; (CH₃)₂SO, 2.50; CH₃CN, 1.93. ESR spectra were obtained on a Varian E-line spectrometer. Spin-trapping experiments with nitrosodurene were performed as previously described.^{1,6} A 200-W Oriol high-pressure mercury arc lamp was used for the photochemical experiments. Corning glass filters (0-52, $\lambda > 350$ nm, 3-73, $\lambda > 430$ nm, 3-71, $\lambda > 470$ nm, and 3-68, $\lambda > 530$ nm) were used to isolate the wavelengths of irradiation. In general, photochemical reactions were monitored by ¹H NMR. Product resonances were identified by comparison with reported spectra and, when possible, with spectra of the compounds in appropriate solvents. In all experiments, the spectrum of a "dark reaction" was recorded as a control. Samples were irradiated in a 15-20 °C water bath. Quantum yields could not be measured because of solid formation during irradiation of Cp₂MoS₂. A rough estimate of the efficiency of the photochemical reactions of Cp₂MoS₂ is 1×10^{-2} - 1×10^{-3} mol/einstein.

Preparation of Cp₂MoS₂ and Cp₂MoS₄. Cp₂MoS₂ was prepared according to the published procedure of Köpf.¹³ Sodium disulfide was prepared from sodium hydrogen sulfide (NaSH) and elemental sulfur in absolute ethanol.¹⁴ Cp₂MoS₄ formed along with Cp₂MoS₂ in this reaction even though care was taken to avoid an excess of sulfur. Cp₂MoS₂ was difficult to isolate by recrystallization since the solubilities of Cp₂MoS₄ and Cp₂MoS₂ are very similar. In addition, Cp₂MoS₂ is slightly unstable at room temperature in solution and forms Cp₂MoS₄. Cp₂MoS₂ was best isolated by sublimation; the yield was extremely low (10-20%) and the sublimation was very slow: only 10-20 mg of Cp₂MoS₂ were obtained after 10 h of sublimation of the crude reaction product at 120-130 °C (0.05-0.1 mm). Cp₂MoS₄ was separated from the crude reaction mixture by flash chromatography on silica gel.¹³ Cp₂MoS₄ was eluted with chloroform as a red-brown solution. (Cp₂MoS₂ decomposed on the silica gel column.¹³) Evaporation of the chloroform from the red-brown fraction yielded red-brown microcrystalline Cp₂MoS₄. The product was recrystallized from acetone. Cp₂MoS₂ and Cp₂MoS₄ were characterized by ¹H NMR (CDCl₃): δ 5.06 (s, Cp in Cp₂MoS₂), 5.24 (s, in Cp₂MoS₄).

(11) Perrin, D. D.; Armarego, W. L.; Perrin, D. R. "Purification of Laboratory Chemicals"; Pergamon Press: Oxford, 1966.

(12) Cooper, R. L.; Green, M. L. H. *J. Chem. Soc. A* 1967, 1155-1160.

(13) Köpf, H.; Hazari, S. K. S.; Leitner, M. Z. *Naturforsch., B: Anorg. Chem., Org. Chem.* 1978, 33B, 1398-1403.

(14) Feher, F. In "Handbook of Preparative and Inorganic Chemistry"; Brauer, G., Ed.; Academic Press: New York, 1963; p 361.

(4) Norman, J. G., Jr. *J. Chem. Phys.* 1974, 61, 4630-4635. Norman, J. G., Jr. *Mol. Phys.* 1976, 31, 1191-1198.

(5) In practice, the program calculates the ratio of atomic radii and varies the percent of the calculated atomic radii while holding the ratio fixed to be used in the molecular potential. Limited computer time necessitates close but non-one virial coefficients. The converged virial coefficient for Cp₂MoS₂ was 1.000 345.

(6) Bruce, M. R. M.; Kenter, A.; Tyler, D. R. *J. Am. Chem. Soc.* 1984, 106 (3), 639-644.

(7) (a) Schwarz, K. *Phys. Rev. B: Solid State* 1972, 5, 2466-2468. (b) Schwarz, K. *Theor. Chim. Acta* 1974, 34, 225-231.

(8) Slater, J. C. *Int. J. Quantum Chem.* 1973, 7, 533-544.

(9) Minimal basis set for Cp₂MoS₂: Mo, $l = 2$; C, $l = 1$; H, $l = 0$; S, $l = 2$.

(10) (a) Müller, A.; Jaegermann, W.; Enemark, J. H. *Coord. Chem. Rev.* 1982, 46, 245-280. (b) Clegg, W.; Mohan, N.; Müller, A.; Neumann, A.; Rittner, W.; Sheldrick, G. *Inorg. Chem.* 1980, 19, 2066-2069. (c) Clegg, W.; Christou, G.; Garner, C. D.; Sheldrick, G. M. *Inorg. Chem.* 1981, 20, 1562-1566. (d) Clegg, W.; Sheldrick, G. M.; Garner, C. D.; Christou, G. *Acta Crystallogr., Sect. B* 1980, B36, 2784-2787. (e) Rittner, W.; Müller, A.; Neumann, A.; Bather, W.; Sharma, R. C. *Angew. Chem., Int. Ed. Engl.* 1979, 18, 530-531. (f) Prout, K.; Cameron, T. S.; Forder, R.; Critchley, S. R.; Denton, B.; Rees, G. *Acta Crystallogr., Sect. B* 1974, B30, 2290-2304.

Irradiation of Cp_2MoS_2 in Benzene. A. A 2.5-mL sample of a 2.7 mM solution of Cp_2MoS_2 in benzene was irradiated ($\lambda > 470$ nm) for 3 h. The solution changed from clear orange to cloudy brown-red. The solvent was removed in vacuo, and the residue was dissolved in CDCl_3 : $^1\text{H NMR}$ δ 5.25 (Cp in Cp_2MoS_4), 5.06 (Cp in Cp_2MoS_2). There are five minor unidentified resonances between δ 6.3 and 5.4, represented by X in Table I. Cp_2MoS_4 also formed in the dark reaction control, but it was less than 2% of Cp_2MoS_2 . **B.** A 1.25-mL sample of a 1.0 mM solution of Cp_2MoS_2 in benzene was irradiated ($\lambda > 350$ nm) for 1 h. The solvent was removed in vacuo, and the residue was dissolved in $(\text{CD}_3)_2\text{SO}$: $^1\text{H NMR}$ δ 5.35 (Cp in Cp_2MoS_4), 5.12 (Cp in Cp_2MoS_2). There are many unidentified resonances in this reaction. Four of these resonances are larger than the resonance for Cp_2MoS_4 : δ 6.32, 6.06, 5.77, and 5.76.

Irradiation of Cp_2MoS_4 in Benzene. A 2.5-mL sample of a 1.0 mM solution of Cp_2MoS_4 in benzene was irradiated ($\lambda > 470$ nm) for 3 h. The solution changed from clear yellow-orange to cloudy brown. The benzene was evaporated in vacuo, and the residue was dissolved in CDCl_3 : $^1\text{H NMR}$ δ 5.28 (Cp in unknown, represented by X in Table I), 5.25 (Cp in Cp_2MoS_4), and 5.06 (Cp in Cp_2MoS_2).

Irradiation of Cp_2MoS_2 in Chloroform-*d*. A 7 mM solution of Cp_2MoS_2 in CDCl_3 (containing 1% C_6H_6) was divided into four equal portions of 0.5-mL each. One of these portions served as the dark reaction, and the other three portions were irradiated for 1 h at (a) $\lambda > 530$ nm, (b) $\lambda > 430$ nm, and (c) $\lambda > 350$ nm. In each of the irradiated solutions some brown solid precipitated. Cp_2MoCl_2 and Cp_2MoS_4 are the major products: $^1\text{H NMR}$ δ 5.61 (Cp in Cp_2MoCl_2), 5.22 (Cp in Cp_2MoS_4), 5.03 (Cp in Cp_2MoS_2). There are eight to ten other resonances in the Cp region (6.2–5.3 ppm) that have not been identified (represented by X in Table I).

Irradiation of Cp_2MoS_4 in Chloroform-*d*. A. A 0.5-mL sample of a 4.6 mM solution of Cp_2MoS_4 in CDCl_3 (containing 0.2% C_6H_6) was irradiated ($\lambda > 530$ nm) for 1.5 h: $^1\text{H NMR}$ δ 5.25 (Cp in unknown, represented by X in Table I), 5.22 (Cp in Cp_2MoS_4), 5.02 (Cp in Cp_2MoS_2). **B.** A 0.5-mL sample of a 7 mM solution of Cp_2MoS_4 in CDCl_3 (containing 0.2% C_6H_6) was irradiated ($\lambda > 350$ nm) for 1.5 h. The solution turned darker and a small amount of brown solid formed. In addition to the products seen in the low-energy irradiation, Cp_2MoCl_2 and some of the same resonances seen in the $\text{Cp}_2\text{MoS}_2/\text{CDCl}_3$ reaction form.

Irradiation of Cp_2MoS_2 in $(\text{CD}_3)_2\text{SO}$. A. A 0.5-mL sample of a 1.4×10^{-2} M solution of Cp_2MoS_2 in $(\text{CD}_3)_2\text{SO}$ was irradiated ($\lambda > 350$ nm) for 1 h: $^1\text{H NMR}$ δ 6.33, 6.21, 6.06, 6.04, 5.78, 5.35 (Cp in Cp_2MoS_4), 5.13 (Cp in Cp_2MoS_2). Cp_2MoS_4 is a minor product relative to the five unidentified resonances between 6.4 and 5.7 ppm. **B.** When a solution of Cp_2MoS_2 in $(\text{CD}_3)_2\text{SO}$ containing 25 equiv of Bu_4NCl was irradiated at $\lambda > 450$ nm or $\lambda > 350$ nm, there was no evidence for formation of Cp_2MoCl_2 (by NMR). The $^1\text{H NMR}$ spectra are similar to the one of Cp_2MoS_2 irradiated in neat $(\text{CD}_3)_2\text{SO}$. A similar experiment was done by using CD_3CN as the solvent. Again, when Bu_4NCl was present in the solution, there was no evidence for formation of Cp_2MoCl_2 in the irradiated solution.

Results and Discussion

SCF- $X\alpha$ -SW Calculations and the Electronic Spectrum. Figure 2 shows the ground-state eigenvalues, symmetries, and primary character of selected Cp_2MoS_2 orbitals. The low-energy electronic transitions will involve transitions between the set of highest occupied molecular orbitals ($14a_1$, $6a_2$, $10b_2$, and $8b_1$) and the set of lowest unoccupied molecular orbitals ($9b_1$, $11b_2$, $7a_2$, and $15a_1$). It is essential to know the character of these orbitals if we are to rationalize the observed photochemistry; the contour plots of the molecular orbitals are helpful in this regard. The highest occupied molecular orbital (HOMO) is the $14a_1$ orbital (Figure 3a). Not unexpectedly for a d^2 complex, this orbital is primarily Mo in character; specifically it is a combination of the $d_{x^2-y^2}$ and d_{z^2} orbitals. The $6a_2$ orbital is next highest in energy (Figure 3b). This orbital is primarily a sulfur π^* orbital. The LUMO orbital is the

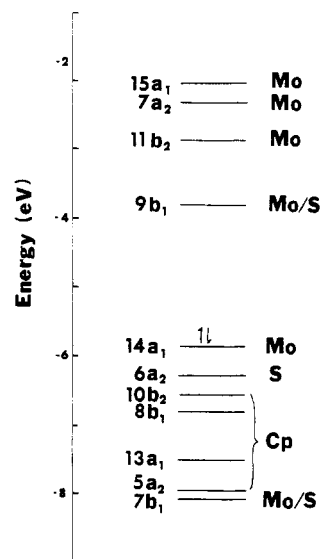


Figure 2. Ground state eigenvalues and primary orbital character for Cp_2MoS_2 .

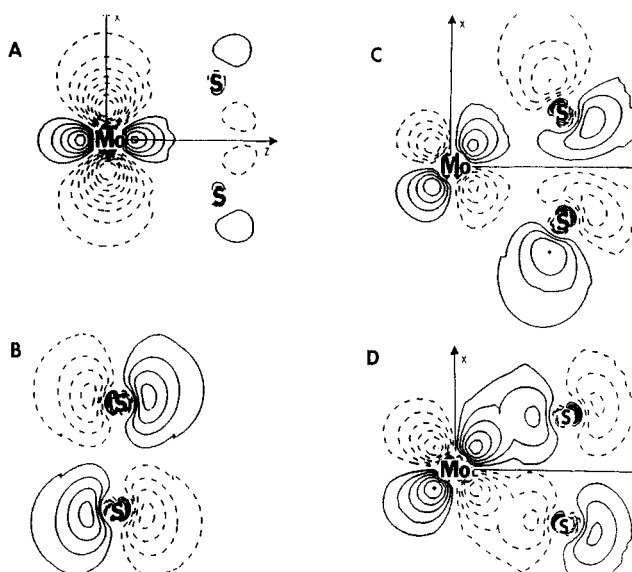


Figure 3. Selected wave function contour plots for Cp_2MoS_2 : A, $14a_1$, xz plane; B, $6a_2$ \perp to xz plane; C, $9b_1$, xz plane; D, $7b_1$, xz plane. Solid and broken lines denote contours of opposite sign at values of ± 0.04 , ± 0.08 , ± 0.12 , ± 0.16 , ± 0.20 , ± 0.24 , ± 0.28 , and ± 0.32 electron $^{1/2}$ $\mu_B^{-3/2}$.

$9b_1$ (Figure 3c). This orbital is a Mo-S antibonding orbital, composed of the d_{zz} orbital on the Mo atom with some p orbital contribution from the S atoms. To slightly higher energy is the $11b_2$ orbital, which is primarily the Mo d_{yz} orbital. To even higher energy is the $7a_2$ orbital, which contour plots show to be primarily the Mo d_{xy} orbital.

In previous calculations on organometallic complexes, we found that the SCF- $X\alpha$ -SW method underestimates the energies of the electronic transitions.⁶ However, the overall pattern of the predicted energies was in good agreement with the experimental values (i.e., all of the predicted energies are red-shifted by the same amount compared to the experimental value). Similar results were obtained in our calculations on the Cp_2MoS_2 complex. The diagram in Figure 4 shows that the calculated transition energies are red-shifted compared to the observed peak maxima, but the pattern of energies is the same for the predicted and experimental values. This agreement between the calculated and experimental values gives us confidence in using the calculated results to assign the

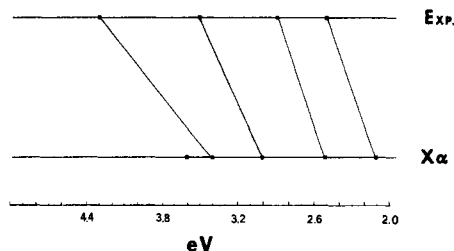


Figure 4. X α transition state vs. experimental transition energies for Cp_2MoS_2 . Only allowed transitions are shown.

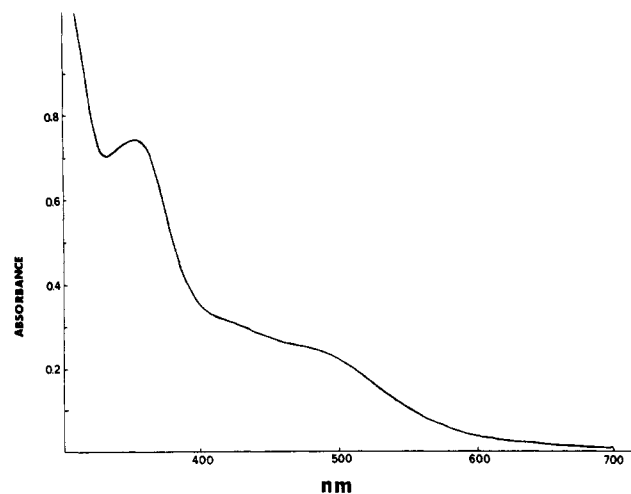


Figure 5. Electronic absorption spectrum of the Cp_2MoS_2 complex in benzene solution (4.5 mM; 1-mm path length; absorbance slidewire set on 0.5).

bands in the electronic spectrum of the Cp_2MoS_2 complex (Figure 5).

Table II summarizes the experimental and calculated electronic transition energies along with their assignments. The important points relevant to the photochemistry of the complexes are these: (1) the band at ≈ 490 nm (assigned as $14a_1 \rightarrow 9b_1$, ${}^1A_1 \rightarrow {}^1B_1$) is a d-d transition (nonbonding d \rightarrow Mo-S antibonding); (2) the band at ≈ 420 nm (assigned as $6a_2 \rightarrow 9b_1$, ${}^1A_1 \rightarrow {}^1B_2$) is a S \rightarrow Mo charge-transfer transition.

Photochemistry. The photochemical reactions of the Cp_2MoS_2 complex are, in general, not "clean". In each reaction, a major product (or products) formed, but there were always other, unidentified products formed in minor amounts (see Experimental Section).¹⁵

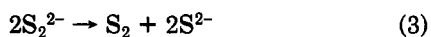
The Cp_2MoS_2 complex reacts photochemically at all absorbing wavelengths in inert solvents to form Cp_2MoS_4 (eq 1). Interestingly, our results also show that the



Cp_2MoS_4 complex converts to the Cp_2MoS_2 complex on irradiation (eq 2).



Equation 1 reveals nothing about the mechanism of Mo-S bond cleavage (heterolytic vs. homolytic) because the disproportionation (3) is known.¹³ Thus, direct ex-



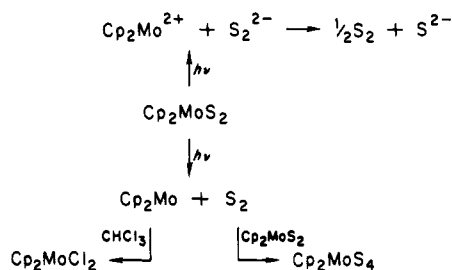
trusion of either S_2 or S_2^{2-} could yield an S_2 molecule

Table II. Experimental and Calculated^a Electronic Transition Energies and Assignments for Cp_2MoS_2

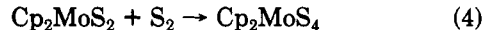
transitn	transitn type ^b	energy, eV	
		calcd	exptl (nm)
$14a_1 \rightarrow 9b_1$ (${}^1A_1 \rightarrow {}^1B_2$) ^c	d \rightarrow d	2.1	2.5 (490)
$6a_2 \rightarrow 9b_1$ (${}^1A_1 \rightarrow {}^1B_2$) ^c	CT (S \rightarrow Mo)	2.5	2.9 (420)
$10b_2 \rightarrow 9b_1$ (${}^1A_1 \rightarrow {}^1A_2$) ^d	CT (Cp \rightarrow Mo)	2.7	
$8b_1 \rightarrow 9b_1$ (${}^1A_1 \rightarrow {}^1A_1$) ^c	CT (Cp \rightarrow Mo)	3.0	3.5 (350)
$14a_1 \rightarrow 11b_2$ (${}^1A_1 \rightarrow {}^1B_2$) ^c	d \rightarrow d	3.0	
$6a_2 \rightarrow 11b_2$ (${}^1A_1 \rightarrow {}^1B_1$) ^c	CT (S \rightarrow Mo)	3.4	4.3 (290)
$14a_1 \rightarrow 7a_2$ (${}^1A_1 \rightarrow {}^1A_2$) ^d	d \rightarrow d	3.5	
$10b_2 \rightarrow 11b_2$ (${}^1A_1 \rightarrow {}^1A_1$) ^c	CT (Cp \rightarrow Mo)	3.6	

^a Spin restricted unrelaxed transition state SCF-X α -SW calculation. ^b Primary character. ^c Electric dipole allowed. ^d Electric dipole forbidden.

Scheme I



capable of reacting with Cp_2MoS_2 to form Cp_2MoS_4 (eq 4).



In order to differentiate between the homolytic and heterolytic pathways, we irradiated the S_2 complex in CDCl_3 . The photochemistry, which was again independent of wavelength, is described by eq 5. We propose that these



reaction products are consistent only with the homolytic extrusion of S_2 from the Cp_2MoS_2 complex. The bottom half of Scheme I shows the proposed pathway while the top half shows the alternative route involving heterolytic extrusion of S_2^{2-} . In the bottom (homolytic) route, S_2 is formed directly and it reacts with Cp_2MoS_2 to form Cp_2MoS_4 . Cp_2Mo , the other primary photoproduct of the reaction, reacts with CDCl_3 to give Cp_2MoCl_2 .^{16,19} (Note

(16) Irradiation of Cp_2MoH_2 in benzene is known to produce H_2 and a form of molybdenocene, $[(\eta^5\text{-C}_5\text{H}_5)_2\text{Mo}(\mu\text{-}\sigma\text{-}\eta^5\text{-C}_5\text{H}_4)_2]$.^{17,18} The latter complex forms by dimerization of the intermediate " Cp_2Mo ". Note that we could not generate " Cp_2Mo " directly from Cp_2MoH_2 in CHCl_3 because Cp_2MoH_2 in CHCl_3 reacts thermally with CHCl_3 to give Cp_2MoCl_2 .¹² The molybdenocene generated in benzene was characterized by ${}^1\text{H}$ NMR and is the same as in ref 18b. Following chromatographic workup to remove unreacted Cp_2MoH_2 , the molybdenocene was dissolved in chloroform-*d*. The proton NMR spectrum shows resonances due to Cp_2MoCl_2 and other unidentified products, and all of the molybdenocene has disappeared.

(17) Geoffroy, G. L.; Bradley, M. G. *Inorg. Chem.* 1978, 17, 2410-2441.
(18) (a) Berry, M.; Davies, S. G.; Green, M. L. H. *J. Chem. Soc., Chem. Commun.* 1978, 99-100. (b) Berry, M.; Cooper, N. J.; Green, M. L. H.; Simpson, S. J. *J. Chem. Soc., Dalton Trans.* 1980, 29-40.

(19) We were unable to identify Cp_2Mo by flash photolysis of Cp_2MoS_2 in THF (1.5×10^{-4} M, 308 nm, Lambda Physik Excimer Laser).²⁰ It is possible that the Mo-S bonds are broken homolytically in a stepwise process to give $\text{Cp}_2\text{Mo}^{\text{III}}\text{S}$. This intermediate could then abstract Cl from CDCl_3 in a stepwise process to give Cp_2MoCl_2 and S_2 , the same products as shown in the homolytic dissociation in Scheme I.

(20) In the flash photolysis of Cp_2MoH_2 in THF, Perutz and Sciano observed a transient attributed to Cp_2Mo . Perutz, R. N.; Sciano, J. C. *J. Chem. Soc., Chem. Commun.* 1984, 457-458.

(15) A variety of complexes can form in low yields when coordinatively unsaturated organometallic complexes and an active elemental form of sulfur are present in solution. See, for example: Vergamini, P. J.; Kubas, G. J. *Prog. Inorg. Chem.* 1976, 21, 261.

that Cp_2MoS_4 is not converted to Cp_2MoCl_2 upon low-energy irradiation in CHCl_3 . Hence, the source of the Cp_2MoCl_2 in this experiment is not Cp_2MoS_4 .) Two points argue against the top (heterolytic) route. First, according to this pathway $\text{Cp}_2\text{Mo}^{2+}$ is an intermediate; it should be possible to trap this species. Yet even with large excesses of Cl^- present, we were unable to observe the formation of Cp_2MoCl_2 when Cp_2MoS_2 was irradiated in $(\text{CD}_3)_2\text{SO}$ or CD_3CN solvent. Second, the steady-state concentration of photoproducted S_2^{2-} will be quite low and consequently it seems unlikely that large amounts of S_2 will form via the (bimolecular) disproportionation process. This factor will tend to limit the amount of Cp_2MoS_4 formed.

It remains to discuss why homolytic extrusion of S_2 occurs when the Cp_2MoS_2 complex is irradiated. By analogy with the d-d band photochemistry of classical coordination complexes, one would expect the S_2 group to be extruded as S_2^{2-} when the complex is irradiated in the $14a_1 \rightarrow 9b_1$ d-d band (490 nm).²¹ The covalency of the Mo-S bond (Figure 3d) may be responsible for the different behavior of the Cp_2MoS_2 complex.²² Of course,

irradiation at higher energy in the $6a_2 \rightarrow 9b_1$ S-Mo CT band (420 nm) is expected to lead to homolytic cleavage: the S_2^{2-} ligand is formally oxidized in the excited state and the Mo center is reduced.

Finally, as might be expected from the results of the calculation, Mo-Cp bond cleavage is not a primary photoprocess with the Cp_2MoS_2 complex. We were unable to observe the nitrosodurene-Cp spin-trapped radical under any of the photolysis conditions described in this paper.

In summary, we can now answer the two questions concerning $\text{S} \rightarrow \text{MCT}$ posed in the introduction to this paper. First, as with the Cp_2TiS_5 complex, $\text{S} \rightarrow \text{MCT}$ excitation in the Cp_2MoS_2 complex leads to homolytic M-S bond cleavage. Second, this behavior is not unique to $\text{S} \rightarrow \text{MCT}$ because d-d excitation of the Cp_2MoS_2 complex also leads to homolytic cleavage and the formation of S_2 .

Acknowledgment is made to the Procter and Gamble Co. for the support of this research through a University Exploratory Research Grant. American Cyanamid is acknowledged for a fellowship to A.E.B.

Registry No. Cp_2MoS_2 , 69228-83-7; Cp_2MoS_4 , 54955-47-4.

Supplementary Material Available: The exact coordinates for the complex (including outer-sphere coordinates) and molecular orbital energies compositions (4 pages). Ordering information is given on any current masthead page.

(21) Zinato, E. In "Concepts of Inorganic Photochemistry"; Adamson, A., Fleischauer, P., Eds.; Wiley-Interscience: New York, 1975; Chapter 4.

(22) An alternative explanation is suggested by Balzani. See: Balzani, V.; Ballardini, R.; Sabbatini, N.; Moggi, I. *Inorg. Chem.* 1968, 7, 1398-1404.

Distortions in Coordinated Cyclopentadienyl Rings: Crystal, Molecular, and Electronic Structural Analysis of (η^5 -Pentamethylcyclopentadienyl)dicarbonylrhodium¹

Dennis L. Lichtenberger,* Charles H. Blevins, II, and Richard B. Ortega

Department of Chemistry, University of Arizona, Tucson, Arizona 85721

Received February 21, 1984

The crystal and molecular structure of $\text{Rh}(\eta^5\text{-C}_5(\text{CH}_3)_5)(\text{CO})_2$ has been determined from a single-crystal X-ray diffraction study. The entire molecule approximates bilateral symmetry with the molecular mirror plane normal to the cyclopentadienyl ring and bisecting the $\text{Rh}(\text{CO})_2$ fragment. The cyclopentadienyl C(ring)-C(ring) bond lengths consist of one short bond of 1.384 (8) Å adjacent to two long bonds of 1.445 (8) and 1.447 (7) Å, with the remaining two bonds having intermediate lengths of 1.412 (8) and 1.410 (7) Å. These bond distances are within one standard deviation of the distances found in the analogous cobalt complex. In addition, the cyclopentadienyl ring exhibits a slight symmetric distortion from planarity that significantly reflects the bonding between the ring and the metal. Molecular orbital calculations on an idealized geometry of $\text{Rh}(\eta^5\text{-C}_5\text{H}_5)(\text{CO})_2$, in which the cyclopentadienyl ring is given D_{5h} symmetry, illustrate the electronic origin of the ring distortion. Calculated three-dimensional electron density maps show that the bonding of the ring to the metal is slightly dominated by a "dialkene" type interaction in which a single e_1^- orbital of the ring donates into an empty inplane metal d orbital of the d^8 $\text{Rh}(\text{CO})_2^+$ portion of the molecule. The distortions of the ring are consistent with the character of this orbital. The title compound crystallizes in the monoclinic space group $P2_1/n$ with $a = 7.765$ (3) Å, $b = 10.741$ (3) Å, $c = 15.267$ (7) Å, $\beta = 98.75$ (3)°, and a calculated density of 1.551 g cm⁻³ for $Z = 4$. Full-matrix least-squares refinement with varying positional and anisotropic thermal parameters for the non-hydrogen atoms and idealized positional and isotropic thermal parameters for the hydrogen atoms converged at $R_1 = 0.0339$, $R_2 = 0.0418$, and GOF = 1.6818 ($n = 136$) for the 1610 independent reflections ($I \geq 3\sigma(I)$) collected with Mo $K\alpha$ radiation over the 2θ range of $4^\circ \leq 2\theta \leq 50^\circ$.

Introduction

The cyclopentadienyl (Cp) ring has played a major role in the development of organometallic chemistry since the discovery of ferrocene in 1951.² A common feature in the

investigation of organometallic chemistry has been the η^5 coordination of a cyclopentadienyl ring to a metal center. The Cp ring has turned out to be a rather versatile ligand and has been observed to coordinate to metal fragments in a number of different σ ,^{3,4} and "slipped" π -bonding

(1) Portions of this work have been presented at the 184th National Meeting of the American Chemical Society, Kansas City, MO, Sept 1982; American Chemical Society: Washington, DC, 1982; INOR 147.

(2) Kealy, T. J.; Pauson, P. L. *Nature (London)* 1951, 168, 1039.